JOURNAL OF SOLID STATE CHEMISTRY 67, 26–36 (1987)

Electrical Properties and Stoichiometry in La_2NiO_4

M. SAYER* AND P. ODIER†

** Department of Physics, Queen's University, Kingston, Ontario, Canada K7L 3N6, and † Centre de Recherches sur la Physique des Hautes Températures, CNRS, 45071 Orleans Cedex 2, France*

Received November 22, 1985; in revised form June 5, 1986

The electrical properties of La_2NiO_4 have been studied with respect to the stoichiometry of the material. The conductivity of reduced compositions has been measured between 20 and 1000 K and compared to that of the air-prepared ones. Nonstoichiometry is present in both cases and produces disorder leading to Anderson localization and to the definition of a mobility edge in the $\sigma_{x^2-y^2}$ itinerant band. Air-prepared compounds contain in addition a large number of Ni^{3+} states which may overlap the itinerant $\sigma_{x^2-y^2}$ band. For reduced materials containing small amounts of Ni^{3+}, the electrical properties can be described below 200 K by a hopping conductivity at the Fermi level within a sharply peaked density of states. The results are well described within the frame of the Mott theory of variable range hopping. Above 200 K highly reduced materials exhibit direct excitation of holes from Ni^{3+} states to the mobility edge in the itinerant band. Under conditions appropriate to air-prepared materials, the Fermi level is shifted toward the itinerant band and a major contribution to the conductivity arises from hopping at the Fermi level. At high temperature a progressive excitation of carriers from the localized states is anticipated with an eventual exhaustion region. This last assumption is corroborated with a shift of the conductivity maximum to higher temperature for increasingly reduced materials.

I. Introduction

La_2NiO_4 fabricated in air has the tetragonal K_2NiF_4 structure shown in Fig. 1 (*1, 2*). This compound is of interest both because of the partially two-dimensional nature of the conduction process (*3–5*) and because a form of semiconductor-to-metal transition is observed at about 600 K; above 600 K, the conduction of both polycrystalline ceramic and single-crystal La_2NiO_4 is "metallic" with a positive temperature coefficient of resistance, below this temperature the conductivity is thermally activated with an activation energy between 0.05 and 0.10 eV (*5, 6*). In the single crystal the transition is reported as being only in the *a–b* plane (*4*).

Goodenough (*5, 7*) has explained the electrical and structural properties of La_2NiO_4 in terms of a band of $\sigma_{x^2-y^2}$ itinerant electron states in the *a–b* plane and localized d_z2 orbitals lying parallel to the *c* axis. Electrons in the latter states are localized because of the relatively weak interactions between the perovskite layers. Arguments supporting this model rest heavily on the evolution of the crystal structure with temperature and in particular on the local distortion of the Ni^{2+} octahedral site, which can be appreciated by the *c/a* ratio of the unit cell. The octahedral distortion passes

† To whom the correspondence should be addressed.

0022-4596/87 $3.00

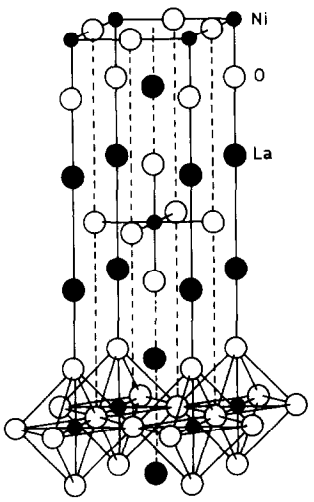

FIG. 1. The ideal K_2NiF_4 structure of La_2NiO_4.

through a maximum at the appearance of the metallic state (*8*) and results from a very short bond between the La and the axial O which can be shortened by substitution of La by Sr (*9*). The appearance of semiconducting properties has been interpreted as resulting from the splitting of the $\sigma_{x^2-y^2}$ band by antiferromagnetic ordering (*10*). However, no such long-range magnetic order has been observed (*11*) and no magnetic or structural transformation has been clearly asociated with the change in electrical properties. In more recent work (*5*) it has been proposed that conduction occurs by a diffusive motion in a $\sigma_{x^2-y^2}$ band which may or may not be split by intra-atomic exchange interactions with localized d_z2 electrons. The observed activation energy is then a motional enthalpy which may be influenced by disorder or polaron formation. In a analogous compound, La_2CuO_4, it has also been suggested that mobile electrons may become trapped in the localized d_z2 orbitals (*5*).

In these arguments, effects due to nonstoichiometry (*6, 10, 11*) have largely been noted but not considered. For example, up to 9–11% of the nickel has been found in the Ni^{3+} state for air-prepared single crystals (*4, 12*) with only 3 to 5% in ceramic samples (*4, 13*).

In terms of the La–Ni–O systems in general, Drennan *et al.* (*14*) have shown that a homologous series of compounds $La_{n+1}Ni_nO_{3n+1}$ exists, the structure of which gives rise to intergrowths for $n > 2$. However, La_2NiO_4 appears to exist as a pure stable phase when its temperature preparation is sufficiently high (*4, 8*). The crystallographic cell is subjected to major changes with composition as evidenced by sensitive variations of c/a with oxygen stoichiometry (*8*). In fact, for samples equilibrated at 1000°C under an oxygen partial pressure of $\sim 10^{-6}$ Pa, the structure changes from that of tetragonal K_2NiF_4 to an orthorhombic structure found in other, but unreduced, mixed rare earth oxides belonging to the K_2NiF_4 family (*15*).

In this paper, we consider the effects of changing oxygen stoichiometry on the electrical conductivity of La_2NiO_4 over the temperature range 20–350 K. Major changes in conductivity are associated with variations in the Ni^{3+} content, and the results are shown to be compatible with carrier hopping or diffusion in the basic band model proposed by Goodenough *et al.* (*5, 10*) but in which an impurity band exists at the band edge. The "metallic" behavior at high temperature can be due either to enhanced phonon scattering in the $\sigma_{x^2-y^2}$ band or to changes in the overall band structure with temperature.

II. Experimental

2.1. Sample Preparation

The pure composition of La_2NiO_4 was prepared by repeated cycles of grinding and firing at 1200°C in air of stoichiometric mixtures of the starting oxides (La_2O_3 and NiO of 3*N* purity). Prior to use, the La_2O_3 and NiO were heated at 1200°C for 24 hr and cooled in a water-free atmosphere. Sintered

material was obtained by isostatic compaction at 400 MPa followed by firing at 1300°C for 48 hr in air. The resulting density was >95% of the theoretical value. A blue coloration on the supporting alumina crucible after sintering indicated some loss of Ni. A brownish color at lower temperature (1000°C) was also visible, and it was further identified to result from interactions between La_2O_3 and alumina. Acceptable sintered material showed only the X-ray diffraction lines of La_2NiO_4 with occasionally a trace of unreacted NiO (*8*).

Cylindrical boules of diameter 0.5 to 1 cm were cut into slices approximately 1 mm in thickness. The resulting disks were equilibrated for 1 hr at 1000°C under argon–oxygen or CO/CO_2 gas mixtures which provided oxygen partial pressures of 2×10^4 Pa (air) to 10^{-7} Pa. Upon completion of the period of equilibration, the sample was caused to fall under gravity to the bottom of the vertical furnace and to cool quickly to room temperature. Samples quenched under an oxygen partial pressure close to that of air retained a dark color. Samples quenched under lower partial pressures took on a brownish appearance which extended throughout the bulk of the sample. All samples were lightly polished to remove surface layers. X-ray powder diffraction spectra made on ground specimens have been described in detail elsewhere (*8*). The c/a ratio for samples indexed as tetragonal (space group I4/mmm-Z = 2) is shown as a function of equilibration oxygen partial pressure in Fig. 2. The c/a ratio decreased with decreasing pO_2 and for the most strongly reduced samples ($pO_2 \sim 10^{-7}$ Pa) the structure became orthorhombic with cell parameters $a = 5.468$ Å, $b = 5.535$ Å, and $c = 12.547$ Å. Reoxidation of reduced samples occurred at above 300°C in air.

The lanthanum and total nickel contents have been chemically analyzed, with the ratio La/Ni being typically in the range of 1.985–1.99 for air-prepared material or for

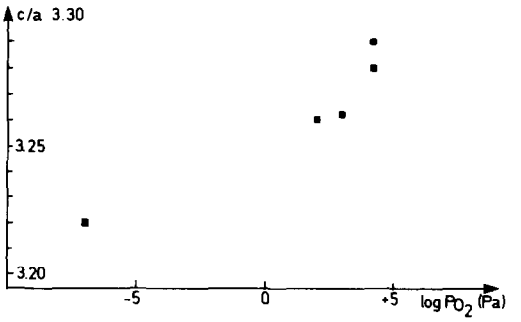

FIG. 2. c/a versus the equilibrating oxygen partial pressure for quenched specimens from 1000°C.

samples equilibrated under $pO_2 \sim 10^{-7}$ Pa. Iodometric titration for Ni^{3+} showed that the proportion of Ni in the Ni^{3+} state was 7 wt% for the air-prepared compound and 0.7 wt% for the reduced one.

2.2. *Electrical*

Electrical conductivity was measured on disk samples by a four-probe Van der Pauw method (*16*). Disks were physically supported by spring-loaded tungsten wires equally spaced around the periphery, and the contact to the sample was completed by a small drop of silver or Pt conducting paint applied at the contact. All solvents were baked off at >100°C prior to measurement. All data were recorded automatically and were independent of the choice of contact pairs. Particularly for air-prepared samples, the absolute value of conductivity was compared with linear four-probe conductivity measurements on La_2NiO_4 bars (*17*). Agreement was achieved between these methods and for different samples to within 10%. Substantial contact effects were, however, noted on all high-conductivity samples, and two terminal measurements were found to be reliable only for the reduced material. Such measurements were employed for the reduced material since electrical leakage in the switching circuit used for the Van der Pauw measurement

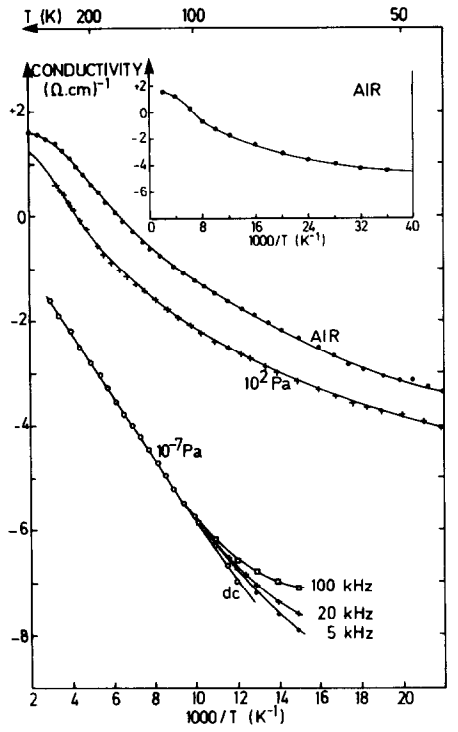

FIG. 3. Low-temperature electrical conductivity for various degrees of reduction. The inset shows the conductivity of the air-quenched material down to 25 K.

was comparable with the sample resistance at the lowest temperature. The effective input of the measurement system was $>10^8$ ohms, and when leakage was detected, the results are corrected for this. For high-temperature measurements (>200°C) platinum contacts were applied using fine platinum wire and platinum paint. In this case the contacts were formed (≥ 800°C) in air before equilibration at a specific pO_2 and no contact problems were observed.

Measurements of the Seebeck coefficient were made by maintaining a temperature differential of <10°C between two copper blocks between which the sample was placed. The sample was generally a disk of about 1 mm in thickness. S was derived from measurements of dE/dT (V/°C) obtained by cycling the temperature within this range. Care was taken to reach an equilibrium temperature prior to each measurement and the results were independent of the type of contacts that were applied. The input impedance of the Keithly 610C electrometer was orders of magnitude higher than the impedance of the sample.

Ac conductivity measurements were made at low temperatures using a helium flow cryostat for $T < 77$ K and liquid-nitrogen-cooled dielectric cells at temperatures >77 K. A three-terminal connection to a General Radio 1615 Capacitance Bridge was the primary measurement tool. Evaporated gold contacts were used and particular care was taken to ensure that the ac data were consistent with the dc measurements at higher temperatures, the derived value of dielectric constant was of reasonable value (~25), and the calculated bulk parameters were independent of sample thickness. While such precautions cannot definitely eliminate the effects of grain boundaries, they provide a reasonable indication that interfacial phenomena are not the determining factor in the measurements.

III. Results

Figure 3 shows log σ versus $1000/T$ for polycrystalline La_2NiO_4 in the temperature range 50–500 K for samples having various degrees of reduction. The inset shows the extension of the temperature range down to 25 K for air-quenched material. In such material the experimental results differed little for a range of specimens prepared at different times. The curve was repeatable for measurement runs made in air and attained a maximum at 55.5 $(\Omega\ \text{cm})^{-1}$ at 620 K. From 150 to 300 K, the log σ versus $1000/T$ plot was reasonably linear, with a conductivity at 300 K of 25 ± 3 $(\Omega\ \text{cm})^{-1}$ and an activation energy of 0.092 ± 0.005 eV. However, the plot is curved at lower temperature giving an activation energy which changes with temperature to 0.01–0.02 eV at 30 K.

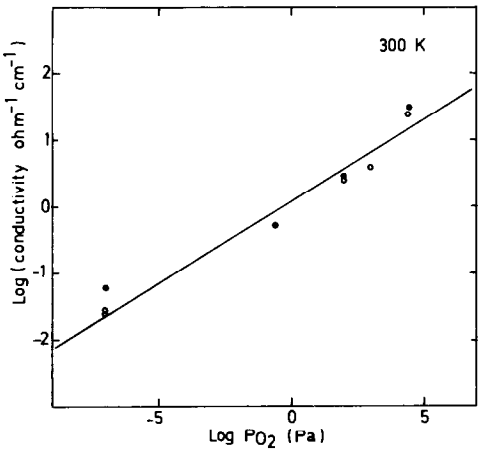

FIG. 4. Conductivity at room temperature versus the equilibrating oxygen partial pressure.

When such samples were reduced the overall conductivity decreased, the initial slope increased to 0.12 ± 0.05 eV, while the lower-temperature curvature was maintained. Upon extreme reduction with $pO_2 \sim 10^{-7}$ Pa, the conductivity at 300 K decreased by a factor of 10^3. A frequency dispersion in the ac conductivity was only observed in the most reduced samples even at the lowest temperature. This may be compared to results obtained for oxides such as $LaVO_3$ (*18*) or VO_2 (*19*) where a significant dielectric dispersion was observed at low temperatures over the same conductivity range as for La_2NiO_4. This would indicate that localization into states having a wide range of energies compared to kT is of major importance in only the reduced La_2NiO_4.

The conductivity measured at 300 K is shown as a function of equilibrium pO_2 in Fig. 4. The relationship can be approximated as $\sigma \sim pO_2^{0.14}$. Evidence that the effect of oxygen stoichiometry is dynamic as well as a function of the quenching process is shown in Fig. 5. Measurements of conductivity were made on samples prepared in air, with temperature increasing into the metallic region. At approximately 1300 K, pure argon was circulated through the chamber and the system was allowed to attain equilibrium. On reduction of the temperature no evidence of a semiconductor–metal transition was present, and the results showed the same general behavior as samples previously quenched in $pO_2 \sim 10^{-7}$ Pa. Details of this process shown in Fig. 6 emphasize that the recovery is not exact. In this case the open circles correspond to a 10^{-7}-Pa sample measured under pure Ar.

Singh *et al.* (*5*) have reported a room-temperature conductivity of about 10 $(\Omega\ \text{cm})^{-1}$ with an activation energy of 0.08 eV. They note a clear break in the conductivity curve at 200 K similar to that exhibited by the 10^2-Pa curve of Fig. 3 of the present work. It is possible that their composition is comparable to that of the material quenched at 10^2 Pa in our work. Rao *et al.* (*4*) report single-crystal conductivities of 0.3 $(\Omega\ \text{cm})^{-1}$ at 300 K and activation ener-

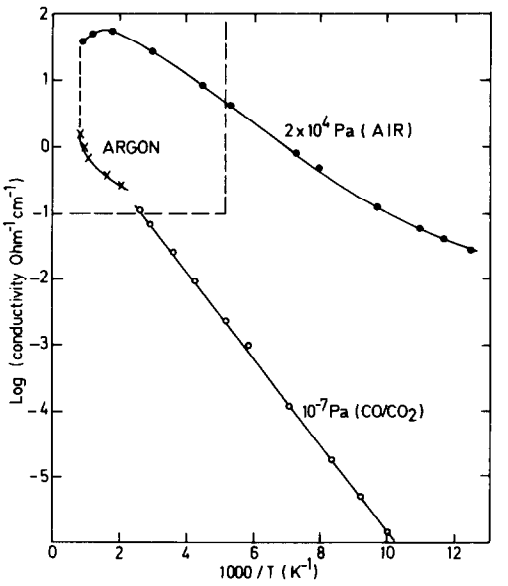

FIG. 5. Electrical conductivity of La_2NiO_4 for various degrees of reduction. ● = La_2NiO_4 measured in air; x = *in situ* reduced and measured under Ar; ○ = measured on a low-pO_2-quenched material.

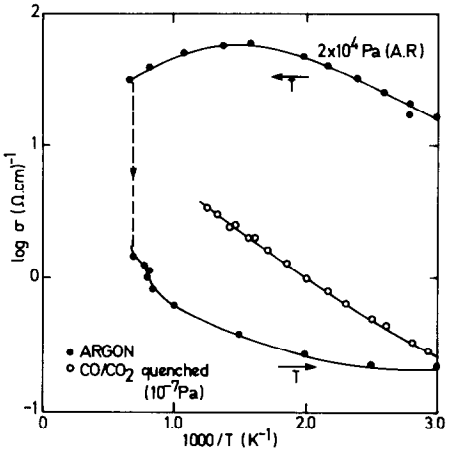

FIG. 6. The high-temperature part of Fig. 5. The conductivity is first measured in air, pure Ar is then circulated at 1300 K, and the conductivity measured during the cooling. ○ = denotes the measurement on a low-pO_2-quenched material measured under Ar flow.

gies between 0.06 and 0.075 eV. Their log σ versus $1/T$ plots are reasonably linear to 100 K.

It is clear that oxygen stoichiometry has a major effect not only on the overall conductivity of La_2NiO_4 but also on the observation of the high-temperature transition. Figure 7 shows measurements of conductivity taken under different pO_2 in the region of the semiconductor–metal transition. The temperature T_E of the onset of "metallic" behavior decreases with increasing partial pressure of oxygen.

IV. Discussion

The crystal structure is expected to lead to a highly anisotropic conductivity. Such an anisotropy should be a feature of measurements on single crystals. However, in measurements on ceramic samples, the results will reflect an average over all crystallographic directions. In the case of La_2NiO_4, this will be very close to that for conduction in the a–b plane.

4.1. Density of States

The model for conduction in La_2NiO_4 proposed by Goodenough *et al.* (*5, 10*) has a primary feature of interelectron correlations induced in a band by intra-atomic exchange coupling with localized d_z2 electrons. This creates a narrowband of itinerant electrons in the a–b plane. Whether or not the $\sigma_{x^2-y^2}$ band is split by a Hubbard gap to give the density of states models shown in Fig. 8a depends upon the size of the interactions. Information concerning these comes principally from the observation of magnetic properties (*5*). These appear to indicate that while a model of strong interactions in an itinerant $\sigma_{x^2-y^2}$ band is substantially correct, at least below 200 K; above this temperature the interactions which may be possibly due to a charge density wave or magnetic interactions (*5, 10, 20*) have either collapsed or have changed their character. On this basis, Singh *et al.* (*5*) have suggested that a diffusion model, possibly including magnetic po-

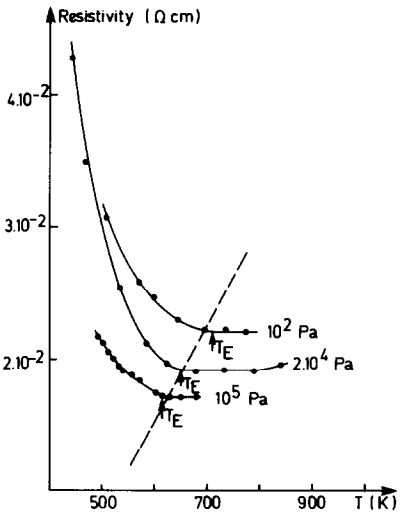

FIG. 7. Evolution of the semiconductor–metal transition temperature with the oxygen partial pressure. T_E denotes the temperature above which the conductivity is metallic.

laron interactions, may be a more appropriate model for the low-temperature conductivity. We review the results of the oxygen stoichiometry in this light.

It is evident that air- or oxygen-prepared La_2NiO_4 contains fairly large amounts of nickel in the Ni^{3+} state (2–12 wt%) depending on whether ceramic material or single crystals are considered (*4*, *12*, *13*). Since this high level of oxidation can be reduced by annealing under low partial oxygen pressure (*4*), nonstoichiometry has to be considered to explain such an observation. From chemical analysis it is found that the ceramic material is lanthanum deficient with a La/Ni ratio of 1.985/1.99. Accordingly, the La^{3+} vacancy (V'''_{La} (if ionized) in the Kroger notation (*21*)) is a possible defect. It is probable that a small amount of La_2O_3 is expelled from the bulk toward the surface during the synthesis of the compound in air. As a consequence, the excess negative charges are compensated by hole states equivalent to Ni^{3+}. The chemical formula for air-prepared material would be approximately $La_{1.985}Ni^{2+}_{0.93}Ni^{3+}_{.07}O_{4.01}$, assuming that very low excess oxygen can be tolerated by the K_2NiF_4 structure. By reduction under low oxygen partial pressure, oxygen vacancies are formed, and this is confirmed by a weight gain after reoxidation of a reduced sample. The oxygen vacancies reduce the Ni^{3+} concentration according to the charge balance:

$$3[V'''_{La}] = h + 2[V^{2\cdot}_{O}]$$

where $V^{2\cdot}_{O}$ represents oxygen vacancies. Thus the Shottky defect involving anion and cation vacancies appears to be of importance in La_2NiO_4. Ni vacancies (V''_{Ni}) could also modify this equation but direct evidence for such defects is not immediately obvious and rather improbable in perovskites. The decomposition pressure for La_2NiO_4 is lower than that in NiO, suggesting a higher stability for Ni–oxygen bonds in this system.

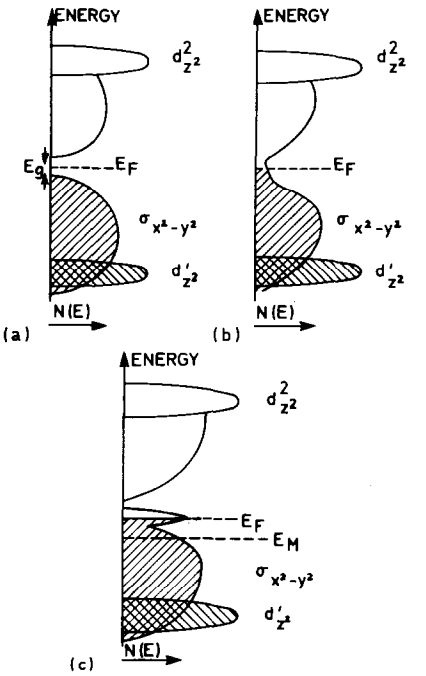

FIG. 8. (a) Density of states versus energy for La_2NiO_4 as proposed in Ref. (*10*) when interactions open a gap. (b) $N(E)$ versus E in the metallic range according to Ref. (*10*). (c) Alternative model for the density of states of an air-quenched La_2NiO_4. A mobility edge is anticipated in the $\sigma_{x^2-y^2}$ and the density of states above that band is associated with Ni^{3+}.

The overall effect of these defects is twofold: (1) the Ni^{3+} hole can be regarded as contributing a carrier to the itinerant band, (2) defects such as V_{La} introduce disorder within this band leading to Anderson localization and the definition of a mobility edge. Even in a fully itinerant band, localized states will exist below the mobility edge and the effective mobility may be further reduced by polaron effects. Thus, even if a Hubbard gap does exist as in Fig. 8a, we anticipate a mobility edge E_m in the $\sigma^*_{x^2-y^2}$ band and a density of states associated with Ni^{3+} lying just above this band. Such a band diagram is shown in Fig. 8c.

Although observations of ordered or line defects have been reported for single-crystal material prepared in air (*14*), no evi-

dence of ordering has been found in reduced material (*22*). On a microscopic basis it is therefore assumed that La vacancies are distributed statistically over La sites. These are clearly capable of producing Anderson localization in the $\sigma_{x^2-y^2}$ band. The strong, but not necessarily direct, correlation between the Ni^{3+} content and the conductivity suggests that states associated with Ni^{3+} interact with itinerant states in the $\sigma_{x^2-y^2}$ band and are not purely associated with localized d_z2 orbitals. If such Ni^{3+} states do play an important role *and* their number is high in air-quenched materials, this would account for the relatively small effect of Sr^{2+} substitution for La^{3+} on the conductivity of $La_{2-x}Sr_xNiO_4$ which has been reported (*9, 13, 23*). The conductivity changes by a factor 2–10 or so for 50% Sr^{2+} substitution in La_2NiO_4 compared with orders of magnitude in systems such as $La_{1-x}Sr_xVO_3$ where the equivalent V^{4+} concentration (playing the same role as Ni^{3+}) is much lower (*24*). Finally, the change in c/a ratio with reduction (decreasing with the Ni^{3+} content) suggests increased electrostatic interaction between Ni and the octahedral oxygens in the c direction which results in a decrease in the NiO bond length in this direction.

4.2. *Low-Temperature Conductivity*

In terms of Fig. 8c, the behavior of a given material will be determined by the relative position of the Fermi level E_F and the mobility edge E_m. Various contributions to the total conductivity may exist, including direct excitation of carriers into itinerant states with energy $\varepsilon = E_F - E_m$ and hopping within the band of impurity states at the Fermi level. If the impurity band is broad due to strong interactions within the material, a clearly defined activation energy leading to a linear log σ vs $1/T$ plot may be difficult to define.

It is of interest that in La_2NiO_4, two contributions do seem to be apparent to the total conductivity (Fig. 3). At low Ni^{3+} content (but still in the tetragonal phase) and at higher temperature, $T > 200$ K, a process with an activation energy of ~0.12 eV exists, where

$$\sigma_1 = \sigma_1(0) \exp^{-\varepsilon_1/kT}, \qquad (1)$$

with the extrapolated conductivity $\sigma_1(0) \sim 3\text{–}5 \times 10^2\ (\Omega\ \text{cm})^{-1}$, neglecting effects from the semiconductor–metal transition. At low temperature ($T < 200$ K) the activation energy varies with temperature, but a crude extrapolation to $1/T \rightarrow 0$ gives $\sigma_2(0) \sim 1\text{–}12\ (\Omega\ \text{cm})^{-1}$. An interpretation of the experimental data in terms of Fig. 8c is that highly reduced material primarily exhibits direct excitation of holes from Ni^{3+} states to the mobility edge in the $\sigma_{x^2-y^2}$ band. Under conditions appropriate to air-prepared material, the Fermi level is shifted toward the itinerant band, and a major contribution arises from hopping at the Fermi level.

If hopping takes place to a mobility edge from a large density of impurity states, the extrapolated conductivity will be defined both by the concentration of carriers in impurity states and also by the mobility in the itinerant band. These two factors do seem to play a role in the high-temperature conductivity region.

If hopping occurs at the Fermi level, one might expect the extrapolated conductivity to equal the minimum metallic conductivity for the system (*25*).

$$\sigma_{min} = 0.026e^2/\hbar a, \qquad (2)$$

where a is the Ni–Ni spacing in the a–b basal plane, $a \sim 3.8$ Å, and $\sigma_{min} = 200\ (\Omega\ \text{cm})^{-1}$. The extrapolation of the conductivity below 200 K gives $1\text{–}10\ (\Omega\ \text{cm})^{-1}$, which appears somewhat small. However, for hopping at the Fermi level, and within a sharply peaked density of states, Mott and Davis (*25*) and Pollak (*26*) have established that a power-law dependence of log σ vs $1/T^n$ should occur, where $n \sim \frac{1}{4}$, such that

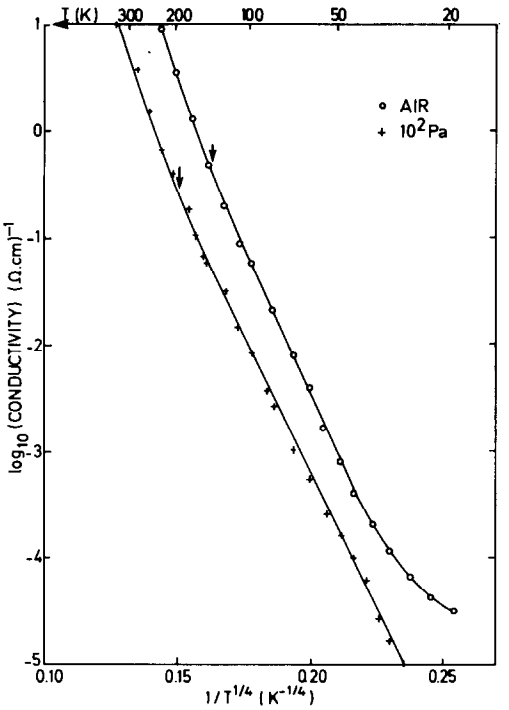

FIG. 9. Log σ vs $T^{-1/4}$ for air-quenched and slightly reduced La_2NiO_4.

$$\sigma(T) = \sigma_2(0) \exp\text{-}B/T^{1/4}. \quad (3)$$

This plot is shown in Fig. 9 for samples quenched in air and at $pO_2 = 10^2$ Pa, respectively. The plot is in reasonable agreement with Eq. (3) from 30 to 200 K, with values for B of 140 and 120 $K^{1/4}$, respectively. Both plots deviate at high temperature and the air-quenched material has a higher conductivity than that predicted at $T = 30$ K. However, the data are consistent with such a contribution to the total conductivity over this relatively large range of temperature.

Mott has shown that for variable-range hopping

$$B = 2.1(\alpha^3/kN(E_F)^{1/4} \quad (4)$$

where α is the decay constant for the carrier wavefunction and $N(E_F)$ is the density of states at the Fermi level. If the effective site spacing is a, then for weak localization $\alpha a < 1$ and the $T^{-1/4}$ dependence should be shown up to a temperature T^* in a system where an energy ε_D is the minimum disorder energy required to describe the process (*18, 25*). These are related by

$$kT^* \geq 1.5\varepsilon_D(\alpha a)^3. \quad (5)$$

If we estimate ε_D from the smallest activation energy measured at low temperature in Fig. 3, ~0.015 + 0.005 eV, it is clear that $T^* \sim 200$ K and Eq. (5) gives $\alpha a \sim 0.9$. With a estimated from the Ni–Ni distance in the a–b plane, $a \sim 3.8$ Å, $\alpha = 0.24$ Å^{-1}. Substituting this in Eq. (4) gives $N(E_F) \sim 10^{19}$ eV^{-1} cm^{-3}. This value is reasonable for such a system.

4.3. High-Temperature Conductivity at the Metal–Semiconductor Transition

Progressive excitation of carriers from localized states to fully itinerant states is anticipated from Fig. 8c, with an eventual exhaustion region at some temperature. The variation in mobility should therefore be a determining factor in the observation of the metal–semiconductor transition, and this is set by scattering within the $\sigma_{x^2-y^2}$ band. The two new observations reported here (Fig. 6) are the disappearance of the transition in heavily reduced material (10^{-7} Pa) and the shift of T_E, the temperature of the conductivity maximum, to higher temperature for increasingly reduced material (Fig. 7). All of these observations are consistent with carrier excitation from localized states into an itinerant band and with the observed change in activation energy resulting from the movement of the Fermi level. Scattering in a strongly interacting electron gas above 600 K then results in metallic behavior as proposed by one of us (*27*) after studies of the plasmon behavior at high temperature in La_2NiO_4 equilibrated under air.

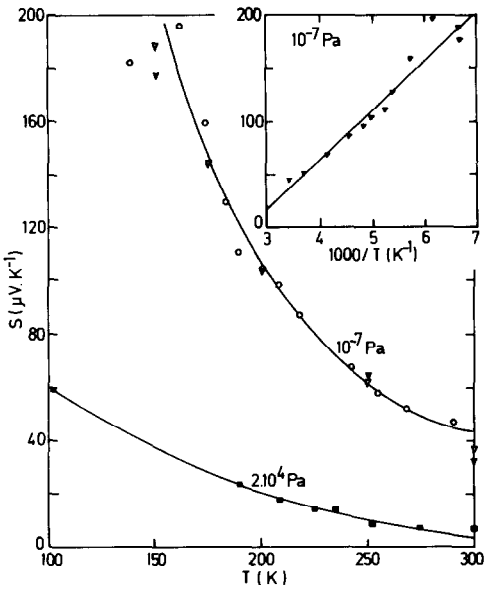

FIG. 10. Seebeck coefficient vs T for air an low-pO_2-quenched La_2NiO_4.

4.4. *Seebeck Coefficient*

Thermopower measurements which have been reported on La_2NiO_4 tend to show a weak ($\sim 10\ \mu V\ K^{-1}$) negative Seebeck coefficient which also changes sign in the interval 300–600 K (*6*). All of these measurements have been made on air-quenched material, and data taken on similar material for $T \sim$ 100–300 K in the present work are consistent with these earlier investigations (Fig. 10), although the sign is positive. Both variability between samples and the change in sign would result from differing contributions to the total conductivity from excitation to the mobility edge in the $\sigma_{x^2-y^2}$ band and hopping at the Fermi energy in the band of impurity states. On the model proposed in this work (Fig. 8c), the density of impurity states is smallest for the most heavily reduced material ($P_{O_2} \sim 10^{-7}$ Pa), and a temperature dependence of the form

$$S = \frac{k}{e}(\varepsilon/kT + A)$$

should be observed, where $\varepsilon \sim (E_m - E_f)$ should be related to the observed conductivity activation energy and A is a constant reflecting the scattering process or a variation of the excitation energy with temperature (*25*). The results for reduced material shown in Fig. 10 and in the inset indeed indicate a much stronger temperature dependence for $S(T)$ than previously reported for air-quenched samples with $E = 0.05$ eV and $A = -1.4$. The observation of an activation energy lower than that of the conductivity activation energy may be an indication of polaron effects (*25*), but it is more likely due to the complexity of the band structure in the region of overlap between the itinerant and impurity bands. The negative value of A, which can be accounted for assuming an excitation energy of the form $\varepsilon(T) = \varepsilon(0) - \gamma T$, where γ is a constant, reinforces this conclusion (*25*).

A small density of states in reduced La_2NiO_4 also translates into a larger range of energies for states compared to kT. The observation of a low-temperature ac conductivity only in reduced material is consistent with this model.

V. Conclusions

The electrical properties of La_2NiO_4 are strongly correlated with the stoichiometry of the system, leading to a band of localized Ni^{3+} states which may overlap a disordered itinerant band. Material prepared in air is highly nonstoichiometric in this sense and La_2NiO_4 with low Ni^{3+} is only achieved by subsequent reduction. If the reduced material is taken as a base, the electrical properties then can be described by the sum of contributions of excitation from impurity levels to a mobility edge and hopping at the Fermi level within the impurity band. This analysis is then comparable to that used for a wide range of other oxides such as $LaCrO_3$ (*28, 29*) and $LaVO_3$ (*18*), and the semiconductor–metal transition is then a func-

tion of exhaustion in the impurity level and scattering in the itinerant band.

Acknowledgments

This work was carried out under the auspices of L'OCTET, a collaborative French–Canadian program in high-temperature materials. Financial support from the National Research Council of Canada and the Centre National de la Recherche Scientifique of France is acknowledged. Discussions with and experimental assistance from Dr. D. S. Smith are appreciated.

References

1. V. Rabenau and P. Eckerlin, *Acta Crystallogr.* **11,** 3094 (1958).
2. H. K. Muller-Buschbaum and V. Lehman, *Z. Anorg. Allg. Chem.* **447,** 47 (1978).
3. L. J. de Jonghe and A. R. Miedema, *Adv. Phys.* **23,** 1 (1974).
4. C. N. R. Rao, D. J. Buttrey, N. Otsuka, P. Ganguly, H. R. Harrison, C. J. Sandberg, and J. M. Honig, *J. Solid State Chem.* **51,** 266 (1984).
5. K. K. Singh, P. Ganguly, and J. B. Goodenough, *J. Solid State Chem.* **52,** 254 (1984).
6. P. Ganguly and C. N. R. Rao, *Mat. Res. Bull.* **8,** 405 (1973).
7. J. B. Goodenough, *Mat. Res. Bull.* **8,** 423 (1973).
8. P. Odier, Y. Nigara, J. Coutures, and M. Sayer, *J. Solid State Chem.* **56,** 32 (1985).
9. M. Khairy, P. Odier, and J. Choisnet, *J. Phys. Colloq., C1,* **42,** C1–831 (1986).
10. J. B. Goodenough and S. Ramasha, *Mat. Res. Bull.* **17,** 383 (1982).
11. P. Ganguly, S. Kollali, and C. N. R. Rao, *Magn. Lett.* **1,** 107 (1980).
12. D. J. Buttrey, H. R. Harrison, J. M. Honig, and R. R. Schartman, *J. Solid State Chem.* **54,** 407 (1984).
13. J. Gopalakrishnan, G. Colsmann, and B. Reuter, *J. Solid State Chem.* **22,** 145 (1977).
14. J. Drennan, C. P. Tavares, and B. C. H. Steele, *Mat. Res. Bull.* **17,** 621 (1982).
15. K. K. Singh, P. Ganguly, and C. N. R. Rao, *Mat. Res. Bull.* **17,** 383 (1982).
16. L. J. Van der Pauw, *Philips Tech. Rev.* **20,** 220 (1958).
17. Y. Nigara, P. Odier, and A. M. Anthony, "Science of Ceramics 11," 551, The Swedish Soc. Ceramics, Stockholm (1981).
18. M. Sayer, R. Chen, R. Fletcher, and A. Mansingh, *J. Phys. C: Solid State Phys.* **8,** 2059 (1975).
19. A. Mansingh, R. Singh, and M. Sayer, *J. Phys. Chem. Solids* **45,** 79 (1984).
20. J. Fontcuberta, G. Longworth, and J. B. Goodenough, *Phys. Rev.* **30,** 6320 (1984).
21. F. A. Kroger, "The Chemistry of Imperfect Crystals," North-Holland, Amsterdam (1974).
22. P. Odier, M. Leblanc, and J. Choisnet, *Mat. Res. Bull.* **21,** 787 (1986).
23. H. W. King, G. J. Murphy, and K. M. Castelliz, *J. Canad. Ceram. Soc.* **52,** 8 (1983).
24. J. B. Webb and M. Sayer, *J. Phys. C: Solid State Phys.* **9,** 4151 (1976).
25. N. F. Mott and E. A. Davis, "Electronic Processes in Non-Crystalline Materials," 2nd ed., Oxford Univ. Press, Clarendon (1975).
26. M. Pollak, *J. Non-Cryst. Solids* **11,** 1 (1972).
27. F. Gervais, Y. Nigara, and P. Odier, *Solid State Commun.* **56,** 371 (1985).
28. D. P. Karim and A. T. Aldred, *Phys. Rev. B.* **20,** 2255 (1979).
29. J. B. Webb, M. Sayer, and A. Mansingh, *Canad. J. Phys.* **55,** 1725 (1975).